Strong Intramolecular Hydrogen Bonding and Molecular Vibrations of 9-Hydroxyphenalen-1-one

Attila Kovács,*,† Vladislav Izvekov,† Károly Zauer,‡ and Koji Ohta§

Research Group for Technical Analytical Chemistry of the Hungarian Academy of Sciences at the Institute of General and Analytical Chemistry, Technical University of Budapest, H-1521 Budapest, Szt. Gellért tér 4, Hungary, Department of Organic Chemistry, Technical University of Budapest, H-1521 Budapest, Szt. Gellért tér 4, Hungary, and Department of Optical Materials, Osaka National Research Institute, AIST, MITI, 1-8-31 Midorigaoka, Ikeda, Osaka 563-8577, Japan

Received: December 14, 2000; In Final Form: February 20, 2001

The strong intramolecular hydrogen bonding in 9-hydroxyphenalen-1-one (**1**) has been investigated by means of quantum chemical calculations and vibrational spectroscopy. Both ab initio molecular orbital (MP2) and density functional theory (B3-LYP, B3-P86) calculations predict a double-minimum potential energy surface with a low (ca. 10 kJ/mol) barrier. The hydrogen-bonding energy, estimated by comparison with the non-hydrogen-bonded anti conformer, is ca. 60 kJ/mol. Our comparative study of the three theoretical levels revealed the very good performance of the B3-LYP density functional in conjunction with a diffuse polarized valence triple-ζ basis set, while the B3-P86 functional tends to overestimate considerably the strong hydrogen-bonding interaction. Based on a joint analysis of the energetics and molecular geometry, the interaction in **1** can be classified as a border case between traditional and short-strong hydrogen bonds. The charge distribution refers to a strong ionic character of the hydrogen-bonding interaction. The vibrational properties of the molecule have been investigated by a combined experimental (FT-IR, FT-Raman) and theoretical analysis. The deficiencies of the computed harmonic force field were corrected by the scaled quantum mechanical (SQM) method of Pulay et al. As a result of our SQM analysis, 45 from a total of 63 fundamentals of the molecule were assigned with an rms deviation of 6.9 cm^{-1} between the experimental and scaled frequencies. The most characteristic effect of hydrogen bonding on the vibrational properties of **1** is the enhanced mixing of the CO and OH vibrations with each other and with the skeletal modes.

Introduction

Hydrogen bonding (HB) is one of the most important of all inter- and intramolecular interactions.[1,2] It is ubiquitous in nature, giving water its unique properties, and playing a key role in the chemistry of living systems. The hydrogen bond arises when a hydrogen atom that is covalently bonded to an electronegative atom (A) interacts with an electron-rich center (B) either in another or in the same molecule, giving rise to a traditional A−H···B hydrogen bond. In this situation, the A−H distance is slightly elongated relative to the A−H distance in a non-hydrogen-bonded form, and the B···H distance is significantly longer than a normal B−H covalent bond distance. A second type of HB has been described as a proton-shared (short-strong or low-barrier) hydrogen bond,[2,3] represented as A···H···B. In this type of bond, the A···H and B···H distances are long relative to the normal A−H and B−H covalent bonds, but the A···B distance is significantly shorter than the A···B distance in a traditional HB. These strong hydrogen bonds can have energies of formation in the gas phase as high as 130 kJ/mol, whereas traditional ones of the type between water molecules are relatively weak (21 kJ/mol or even weaker in the gas phase).[2]

The study of strong HB is an area of active research. Besides the numerous examples in inorganic and organic materials,[3−12] they have been lately shown to exist in a high-pressure phase of ice.[13,14] They have also been suggested to contribute in enzyme-catalyzed reactions, although, lacking direct experimental evidence, this role is still controversial.[15−19]

While most strong hydrogen bonds involve charged fragments, keto−enols constitute an intriguing set of compounds that form strong intra- and intermolecular hydrogen bonds in which nominally no charges are involved.[20] Such strong O−H···O hydrogen bonds are believed to exist when the O···O distance is below 2.5 Å. These very short distances are accompanied by a significant lengthening of the O−H covalent bond and a shorthening of the O···H hydrogen bond up to a near symmetrical arrangement at an O···O distance of ca. 2.40 Å. To rationalize the short hydrogen bonds in these conjugated neutral systems, Gilli et al. have proposed the resonance-assisted hydrogen-bonding model linking the strength of the hydrogen bond to the resonance in the keto−enol system.[21,22] In this model two energetically equivalent valence bond resonant forms can exist, leading to a short strong hydrogen bond. The corresponding stabilization by resonance is the factor that permits one to overpass the steep increase of the interatomic repulsion term as the O···O distance shortens.

A characteristic representative of keto−enols with strong HB is the 9-hydroxyphenalen-1-one molecule (**1**) carrying a hydroxy group at a peri position to a carbonyl group (Figure 1). The

* Corresponding author. Fax: (361)-463-3408. E-mail: attila@tki.aak.bme.hu.

† Institute of General and Analytical Chemistry, Technical University of Budapest.

‡ Department of Organic Chemistry, Technical University of Budapest.

§ Osaka National Research Institute.

10.1021/jp0045033 CCC: $20.00
Published on Web 04/28/2001

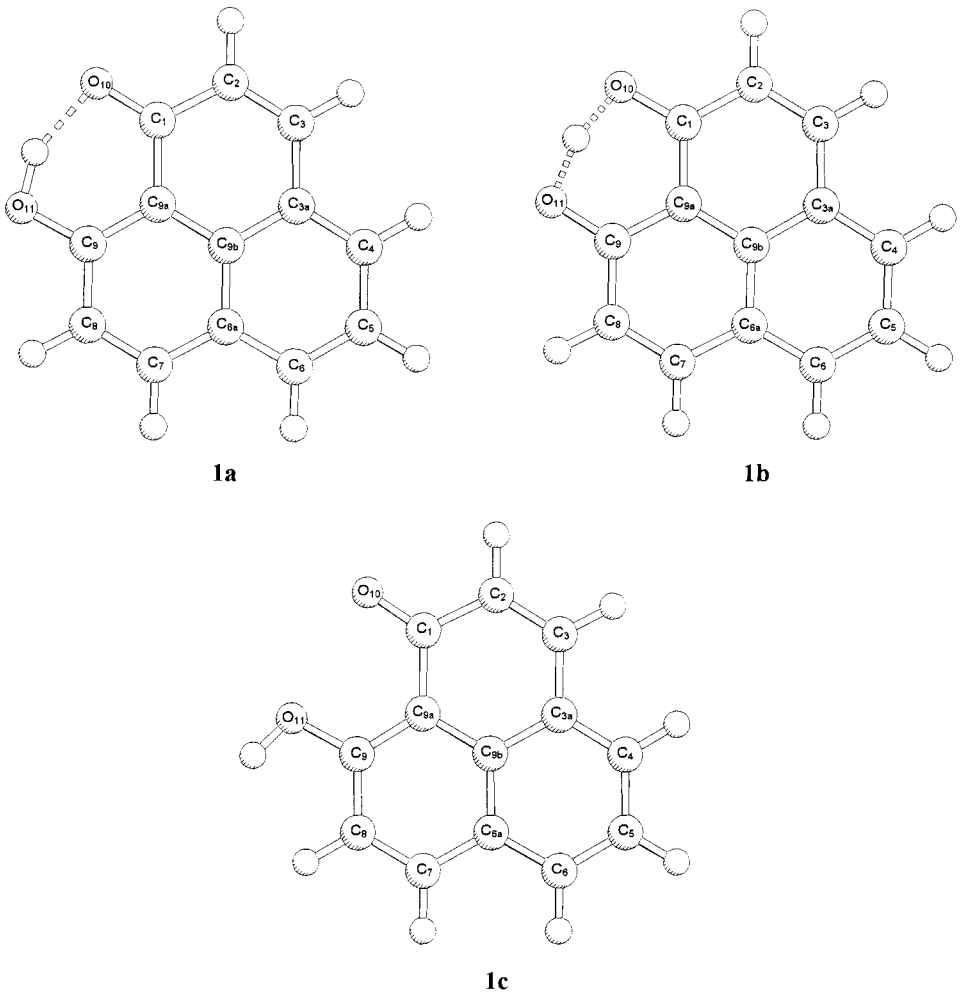

Figure 1. Molecular geometry and numbering of atoms in the three characteristic structures of 9-hydroxyphenalen-1-one (**1**).

chemical behavior of the compound is known to be anomalous both as a phenol and a ketone because the hydroxyl group can be neither acetylated nor methylated and the carbonyl group affords no oxime or Schiff bases. This behavior can be attributed to the strong conjugated HB between the two groups evidenced by the short O···O distance (<2.5 Å[23]) and the lack of the O−H stretching band in the IR spectrum.[24] X-ray crystallography at 298 K[23,25] and ^{1}H and ^{13}C NMR studies[26,27] indicated either that the hydrogen bond is symmetric (Figure 1, **1b**) or that a rapid interconversion occurs between two asymmetrically hydrogen-bonded structures being the mirror image of each other (Figure 1, **1a**). X-ray photoelectron,[26] deuteron quadrupole,[28] and vibronically resolved laser-excited fluorescence studies as well as fluorescence excitation in an argon matrix at 4 K[29] supported the asymmetric hydrogen bond and the intramolecular proton exchange between two equivalent tautomers. The tunneling frequency of the proton has been determined to be 69 cm^{-1} for the ground state.[30] The hydrogen tunneling dynamics in **1** was investigated in several additional studies.[31−34] The barrier for the double minimum potential was estimated to be 21.7 kJ/mol using HF/STO-3G calculations,[31] while recently a value of 31.9 kJ/mol was suggested on the basis of a combined theoretical (HF/6-31G**) and experimental (fluorescence excitation) analysis.[34] In both studies the HF optimized geometries were used, which, however, may not have the necessary reliability due to the deficiencies of these low-level calculations. Additionally, the latter study indicated substantial structural reorganizations between the equilibrium configuration and the transition state.[34] Hence the heavy-atom movement plays a significant role in the hydrogen transfer and the exact knowledge of this structural reorganization and that of the normal modes are of paramount importance to complete our information on the tunneling dynamics in **1**.

In the present study we investigate the energetic, structural, and vibrational characteristics of the intramolecular HB in 9-hydroxyphenalen-1-one by means of quantum chemical calculations and vibrational spectroscopy. All the three characteristic structures of **1** (**1a**, **1b**, and the non-hydrogen-bonded planar conformer **1c**, cf. Figure 1) are considered. We selected the second-order Møller−Plesset theory (MP2)[35] in conjunction with a diffuse polarized split-valence triple-ζ basis set as the primary computational level in our study. Because of its reliability, this and similar levels are generally accepted for investigation of HB interactions.[36−38] In addition we investigate the performance of popular density functional theory (DFT) methods for describing the present strong HB system. The molecular vibrations of **1** are determined by a combined experimental and theoretical analysis with a particular interest on the effect of the strong HB on the normal modes.

Previous theoretical investigations of the intramolecular HB in **1** include the above-mentioned two HF studies[31,34] as well as several semiempirical calculations using the INDO, MNDO, and AM1 methods.[39−41] Similarly, only preliminary information is available on the vibrational characteristics of **1**: the absence of the OH stretching band as well as the assignment of the CO stretching bands in the infrared spectrum were reported,[24,42] while some fundamental frequencies in the far-IR range were measured by high-pressure Raman spectroscopy.[43]

Computational Details

Calculations of the molecular geometries and energetics of the three structures **1a**−**c** were carried out using the second-order Møller−Plesset perturbation theory (MP2)[35] and the Becke3−Lee−Yang−Parr (B3-LYP)[44,45] and Becke3−Perdew86[44,46] exchange-correlation functionals. In all the calculations the 6-311G** basis set was used. To account properly for the HB interaction, the basis sets of the oxygens and the OH hydrogen were extended with a single set of diffuse functions. This basis set is denoted in the following as 6−311(++)G**. The calculations were carried out using the GAUSSIAN 98 suite of programs.[47] The minimum character of structures **1a** and **1c**, and the first-order saddle-point character of **1b** was confirmed by B3-LYP frequency calculations. The zero-point vibrational energy (ZPE) corrections to the absolute energies were taken from these B3-LYP calculations and were used without scaling.

Our vibrational analysis is based on the computed B3-LYP harmonic force field. This choice is reasoned by the good agreement found between the present MP2 and B3-LYP results (vide infra). The deficiencies of the computed harmonic force field were corrected by the scaled quantum mechanical (SQM) method of Pulay et al.[48] The Cartesian representation of the theoretical force constants has been computed at the fully optimized geometry. The SQM analysis was performed in the internal coordinate representation using a nonredundant set of primitive internal coordinates. The Cartesian force field was transformed to internal space by the program TRA3.[49] For the scaling scheme Pulay's standard (selective) scaling method[50] was used, in which the computed harmonic force constant matrix F has to be subjected to the congruent transformation $F' = T^{1/2}FT^{1/2}$, where F' is the scaled force constant matrix and T is the diagonal matrix containing the scale factors t_i. The atomic masses used for generation of the inverse kinetic energy matrix, G, were as follows: H, 1.0078; C, 12.011; O, 15.999 (in atomic mass units). Scaling of the theoretical force field and solution of the secular equation were done with the program SCALE3.[51,52] The quality of the SQM data was assessed by the root-mean-square deviation between the experimental and SQM frequencies. For characterization of the fundamentals their total energy distribution (TED)[53,54] was used, which provides a measure of each internal coordinate's contribution to the normal coordinate in terms of energy.

Experimental Section

The sample was prepared by a slight modification of the original method of Koelsch and Anthes[55] in order to obviate the isolation of the intermediate 1-cinnamoyl-2-methoxynaphthalene. Cinnamoyl chloride (19.8 g) and 2-methoxynaphthalene (22.0 g) were dissolved in 200 cm^3 of dry 1,2-dichloroethane. After cooling, 18.0 g of dry $AlCl_3$ was added slowly (within 5 min) while the solution was mechanically stirred. After stirring for 60 min and cooling again, a further 18.0 g of $AlCl_3$ was added. The solution was stirred at room temperature for 8 h and in an oil bath at 100 °C for additional 3 h, whereupon the mixture started to turn into a solid. At that point the reaction was quenched by pouring into a mixture of ice (150.0 g) and hydrochloric acid (80 cm^3). The aqueous mixture was repeatedly extracted with methylene chloride (2 × 200 cm^3) and ethyl acetate (2 × 100 cm^3). The organic phase was dried over $MgSO_4$ followed by evaporation of the solvents. The residue (17.1 g; 73.8%) was sublimed in a vacuum (0.5 Torr) in an oil bath at 200 °C. Yield 12.6 g (54.4%); mp 191 °C. After recrystallization from methanol: mp 201−202 °C (lit. mp 200−201 °C[55]).

Solution and solid-phase infrared spectra were recorded on a Perkin-Elmer System 2000 Fourier transform IR spectrometer equipped with an MCT detector for the mid-IR range and with a DTGS detector for the far-IR range. The liquid-phase spectra were recorded using 0.05 M CCl_4 solution[56] in 0.22 mm KBr and 1.0 mm polyethylene liquid cells for the 4000−450 and 450−100 cm^{-1} ranges, respectively. The spectra of the solid were measured using KBr (mid-IR) and polyethylene (far-IR) pellets. Measurements in the gaseous phase were hindered by the low vapor pressure of **1**.[29] The number of scans accumulated with the solid and solution samples were 16 (mid-IR) and 128 (far-IR), respectively. The spectra were recorded using a resolution of 4 cm^{-1}.

The Raman spectra were measured in the 4000−150 cm^{-1} range with a Nicolet Model 950 FT-Raman spectrometer at 2 cm^{-1} resolution using the 1064 nm line of a Nd:YAG laser for excitation (at 100−600 mW output power) and 180° scattering geometry. In general, 512 scans were co-added. The solvent spectra were subtracted from those of the solution measured under the same conditions. Our efforts to perform depolarization measurements failed because of the low solubility of **1** in nonpolar solvents.

Results and Discussion

1. Energetics and Geometrical Characteristics of the Strong Hydrogen Bonding. The character of the three stationary points on the potential energy surface (PES) of **1** was determined to be the following: the asymmetric hydrogen-bonded form (**1a**, cf. Figure 1) is the global minimum and the symmetric (C_{2v}) hydrogen-bonded form (**1b**) is a low-lying first-order saddle-point, while the non-hydrogen-bonded form with the hydroxy hydrogen oriented opposite to CO_{10} (**1c**) is a local minimum. All the three structures are planar, confirming the results of previous structural studies.[23,31,34,39−41] Our following discussion of the energetics and molecular geometries of **1a**−**c** is based on the MP2 calculations, which level was shown to be sufficiently reliable for these properties of HB systems.[36−38] The DFT results will be discussed shortly, focusing on their performance on the strong HB interaction as compared with the "reference" MP2 data.

The relative energies of the three structures obtained at various levels of theory are compiled in Table 1. The relative energy of **1c** with respect to **1a** provides us an estimate of the HB energy. The MP2 value of ca. 65 kJ/mol refers to a very strong hydrogen bond,[1,3] but it is still well below the stabilization energies of low-barrier hydrogen bonds found in anionic systems (ca. 100 kJ/mol[11,57]). This large stability of the **1a** conformer is in agreement with previous experience that the **1c** structure has no chemical relevance under common experimental conditions.

The zero-point vibrational energy (ZPE) corrections exert only a minor influence on the calculated relative energies of the **1a** and **1c** forms (cf. Table 1). We note the probable larger error of the ZPE of **1a** because of the expected strong anharmonic character of the OH stretching mode in this conformer and the consequently larger overestimation of this frequency by the harmonic approximation used in the computations.[38] The calculated ZPE of **1b** should be treated with even more caution, because the fundamental associated with the imaginary frequency (containing mainly the motion of the enol hydrogen) is coupled with several other normal modes affecting their frequencies. Nevertheless, the adiabatic potential energy barrier is decreased at all the levels of theory as compared to the classical proton transfer energy barrier but definitely still has a positive value at the MP2 level.

TABLE 1: Energetics, Geometrical and Charge Characteristics of the Strong Hydrogen Bonding in 9-Hydroxyphenalen-1-one[a]

	MP2			B3-LYP			B3−P86		
	1a	**1b**	**1c**	**1a**	**1b**	**1c**	**1a**	**1b**	**1c**
ΔE	0.0	12.0	63.3	0.0	10.2	70.2	0.0	6.3	75.0
ΔE_{ZPE}[b]	0.0	1.9	61.7	0.0	0.1	68.6	3.8	0.0	77.2
$O_{10}\cdots H_{OH}$	1.618	1.202		1.612	1.209		1.545	1.204	
$O_{10}\cdots O_{11}$	2.543	2.369	2.647	2.535	2.375	2.664	2.491	2.366	2.648
$O_{11}-H$	1.000	1.202	0.964	1.006	1.209	0.964	1.018	1.204	0.963
$O_{10}\cdots H-O_{11}$	151.7	160.5		150.1	158.3		152.4	158.7	
$C_9-O_{11}-H$	104.9	101.3	107.7	106.1	102.5	109.2	105.2	102.2	109.0
$q(O_{10})$	−0.765	−0.773	−0.658						
$q(O_{11})$	−0.754	−0.773	−0.691						
$q(H_{OH})$	+0.536	+0.532	+0.464						
$q(C_1)$	+0.642	+0.624	+0.618						
$q(C_9)$	+0.561	+0.624	+0.507						
$q(C_{9a})$	−0.301	−0.327	−0.242						
$q(C_2)$	−0.290	−0.296	−0.265						
$q(C_3)$	−0.066	−0.048	−0.106						
$q(C_7)$	−0.057	−0.048	−0.069						
$q(C_8)$	−0.283	−0.296	−0.303						

[a] The relative energies are given in kJ/mol, the distances in Å, and the angles in deg. The natural charges (q) were obtained using the NBO scheme.[62] In all the calculations the 6−311(++)G** basis set was used, for details see text. [b] Relative energies corrected by zero-point vibrational energy (ZPE). The ZPE corrections were obtained from the B3-LYP calculations and were used without scaling.

The relative energy of **1b** with respect to **1a** represents the barrier height between the two minima of the symmetric double potential well. This parameter, together with the interminimal distance, is of paramount importance in the description of the hydrogen tunneling dynamics in low-barrier HB systems. Previous experimental and theoretical estimates range from 20 to 80 kJ/mol[29,31,34] for the barrier height in **1**. One of the most crucial deficiencies of these earlier studies was, however, the inadequacy of the used interminimal distance, which is known to be very important for determining the barrier height.[58] The present MP2 calculations predict this distance to be 0.637 Å. In earlier studies values of 0.4 Å (from X-ray analysis[23]) and 0.82 Å (from HF/6-31G** calculations[34]) were utilized, being in considerable error with our, undoubtedly the most reliable, value. The best agreement with the present calculated barrier height (12.0 kJ/mol) was published by Kunze and de la Vega: they obtained 21.7 kJ/mol for the barrier height and 0.64 Å for the interminimal distance using HF/STO-3G calculations.[31]

Another deficiency in the early studies of the tunneling dynamics was the used simple one-dimensional model neglecting a coupling of the proton tunneling motion with the rearrangement of the carbon−oxygen framework.[29,30,32,33] In fact, the proton tunneling is a multidimensional phenomenon due to the vibrations of the keto−enol skeleton. Hence the barrier is not static but oscillates with the frequency of these atomic motions. Utilizing the present calculated geometrical parameters in conjunction with a direct dynamics method for proton tunneling,[34] a properly accurate value of the barrier height might be obtained.

Assessment of the three theoretical levels used in the present study shows some overestimating character of DFT for the strength of HB in **1** with respect to MP2 theory. This is manifested in both the larger HB energies and lower barrier heights obtained at the DFT levels (cf. Table 1). The performance of DFT for HB systems has been investigated in several studies reporting considerable overestimation when utilizing double-ζ basis sets.[36,59,60] In the case of the B3-LYP functional the increase of the basis set (up to diffuse valence triple-ζ quality) was suggested to overcome this deficiency.[37] This enhanced level worked well also for the strong hydrogen bond in nitromalonamide.[61] Less information is available for the B3-P86 functional. A comparative study on the strong HB in the hydrogen maleate ion using the B3-PW91 functional (known to give close results to those of B3-P86) with a valence double-ζ basis set showed an overestimating character of B3-PW91 with respect to MP2 and B3-LYP.[11] Our present study indicates the insufficiency even of a diffuse valence triple-ζ basis in conjunction with the B3-P86 functional. As the most obvious consequence of the overestimating character of B3-P86, this adiabatic potential energy barrier becomes negative (cf. Table 1). On the other hand, the B3-LYP results show only negligible overestimation with respect to MP2.

The above conclusions are supported by the calculated molecular geometries. The most important geometrical characteristics of HB obtained by the three methods are summarized in Table 1. Inspecting the **1a** structures, the $O_{10}\cdots H_{OH}$ and $O_{10}\cdots O_{11}$ distances from the B3-P86 calculations are shorter by 0.07 and 0.05 Å than the respective MP2 distances while the deviations of the B3-LYP results from the MP2 ones are much smaller (0.006 and 0.003 Å, respectively). On the other hand, the geometrical characteristics of both the symmetric hydrogen-bonded (**1b**) and the non-hydrogen-bonded conformers (**1c**) calculated by the three methods are in excellent agreement! This agreement found for the **1c** structure reflects the generally observed good performance of the B3-LYP and B3-P86 functionals in structural studies of common organic compounds.

The natural charges[62] give us important information on the variation of charge distribution upon the HB interaction in **1** (cf. Table 1). As compared with the non-hydrogen-bonded conformer **1c**, the electron density is considerably increased on both the proton donor (0.06 e) and acceptor oxygens (0.11 e) parallel with a charge decrease on the OH hydrogen in **1a**. The increased charge separation in the CO bonds is reflected on the respective carbons (C_1 and C_9) as well. These data point both to the strong ionic character of the HB interaction and to the enhanced electrostatic character of bonding within the $-C_1-O_{10}\cdots H-O_{11}-C_9-$ moiety in **1a**. Somewhat smaller, but characteristic changes can be seen on C_{9a} as well as on the two (formally double) CC bonds C_2-C_3 and C_7-C_8. The overall electrostatic picture of the two forms shows that the charge increase on O_{11} in **1a** originates from the $C_7-C_8-C_9$ moiety, while that of O_{10} is transferred mostly from the OH hydrogen.

The atomic charges of **1a** and **1b** indicate a very similar electron density distribution in the two hydrogen-bonded conformers. The most important feature is the unchanged strong electrostatic character of the HB interaction in the symmetric

hydrogen bond (**1b**). The differences are generally within 0.02 e; The only noteworthy exception is C_9 losing 0.06 e which covers the electron density enhancement of the neighboring O_{11} and C_{9a}. The marginal differences in the charge distribution of **1a** and **1b** are in agreement with observations on other strong HB systems.[10]

The most important geometrical characteristics of HB are the hydrogen bond length ($O_{10}\cdots H$) and the nonbonded $O_{10}\cdots O_{11}$ distance. Based on a comparison with available literature data of various hydrogen-bonded systems they can also be used to characterize the strength of HB interactions. In the literature the following geometrical criteria are used for strong HB: O···H < 1.5 Å and O···O < 2.5 Å.[1,3] The two distances in **1a** (1.618 and 2.543 Å, respectively) nearly reach these criteria. These distances agree with those found in crystalline carboxylic acids[63−67] classified as the strongest within traditional hydrogen bonds. On the other hand, the calculated HB energy in **1a** (63 kJ/mol being over the accepted criterion of 40 kJ/mol[4]) and the experimentally well-established hydrogen tunneling resemble the properties of short-strong low-barrier hydrogen bonds. Seemingly, **1a** represents a border case between traditional and short-strong hydrogen bonds.

It is noteworthy that the ratio of the calculated O···H and O···O distances in **1a** fit satisfactorily in the correlation diagram evaluated by Ichikawa[68] on the basis of X-ray and neutron diffraction data of 79 hydrogen-bonded molecules.

Another useful point on the characteristics of the HB in the present keto−enol system can be gained from a comparison with simple intermolecular C═O···HO hydrogen-bonded systems. For this assessment we chose the $H_2C{=}O\cdots H_2O$ and $H_2C{=}O\cdots HOCH_3$ dimers for which the calculated MP2/6−311-(++)G** geometrical and energetic properties are O···H distances 2.021 and 2.022 Å, O···O distances 2.887 and 2.895 Å, and HB energies 22.1 and 22.3 kJ/mol, respectively. With these parameters the above dimers belong obviously to medium-strong traditional HB interactions.[1,2] The much shorter O···H distance and the much larger HB energy in **1a** (vide supra) demonstrate the effects of resonance[21,22] in the present keto−enol system. We should note also another possible cooperative effect: that of the steric intramolecular constraints. A steric compression may contribute to the shortening of the O···H and O···O distances in **1a**, which effect, however, would decrease the HB energy. The found HB energy in **1a** refers to a small influence of these steric interactions.

The effects of HB on the molecular geometry can be best evaluated by comparing the geometrical parameters of the two hydrogen-bonded forms **1a** and **1b** with those of the non-hydrogen-bonded **1c** structure (cf. Table 2). The parameter most sensitive on HB is the O−H bond length, where the lengthening of the bond upon the interaction can be related to the strength of the hydrogen bond. In the case of **1a** this lengthening amounts to 0.036 Å, considerably larger than found in the intermolecular $CH_2O\cdots HOCH_3$ interaction (0.005 Å). At the same time the $C_1{-}O_{10}$ bond of **1a** lengthens by 0.023 Å while the $C{-}O_{11}$ bond shortens in a similar amount. All these changes are in agreement with the resonance character of this tautomeric system; that is, the **1a** structure reflects the features of its tautomer counterpart. A similar conclusion can be drawn from the change of the bond distances in the carbon skeleton: here the shortening of the formally single $C_1{-}C_2$ and $C_1{-}C_{9a}$ bonds is the most significant (by 0.016 and 0.030 Å, respectively), but the variation of the other skeletal bonds (shorter $C_3{-}C_{3a}$, longer $C_2{-}C_3$, $C_{6a}{-}C_7$, $C_8{-}C_9$, $C_9{-}C_{9a}$) corresponds to the resonance model as well, only the magnitudes are smaller (<0.01 Å). All these changes reflect an increased conjugation upon hydrogen bonding in the $C_1\cdots C_{9a}$ ring.

TABLE 2: Selected Geometrical Parameters of the Three Characteristic Structures of 9-Hydroxyphenalen-1-one[a]

Bond Lengths (Å)			
	1a	**1b**	**1c**
$C_1{-}C_2$	1.458	1.439	1.474
$C_2{-}C_3$	1.363	1.372	1.355
$C_3{-}C_{3a}$	1.446	1.438	1.449
$C_{3a}{-}C_4$	1.399	1.407	1.395
$C_4{-}C_5$	1.405	1.399	1.408
$C_5{-}C_6$	1.390	1.399	1.385
$C_6{-}C_{6a}$	1.415	1.407	1.419
$C_{6a}{-}C_7$	1.427	1.438	1.418
$C_7{-}C_8$	1.377	1.372	1.377
$C_8{-}C_9$	1.421	1.439	1.418
$C_9{-}C_{9a}$	1.408	1.427	1.403
$C_{9a}{-}C_{9b}$	1.423	1.416	1.431
$C_{3a}{-}C_{9b}$	1.425	1.423	1.429
C_{6a}-C_{9b}	1.426	1.423	1.430
$C_1{-}C_{9a}$	1.463	1.427	1.493
$C_1{-}O_{10}$	1.255	1.291	1.232
$C_9{-}O_{11}$	1.332	1.291	1.355
$O_{11}{-}H$	1.000	1.202	0.964
$C_2{-}H$	1.086	1.086	1.087
$C_3{-}H$	1.089	1.089	1.089
$C_4{-}H$	1.088	1.088	1.088
$C_5{-}H$	1.086	1.086	1.086
$C_6{-}H$	1.088	1.088	1.088
$C_7{-}H$	1.088	1.089	1.088
$C_8{-}H$	1.086	1.086	1.090
Bond Angles (deg)			
	1a	**1b**	**1c**
$C_1{-}C_2{-}C_3$	121.4	120.4	122.6
$C_2{-}C_3{-}C_{3a}$	122.0	122.0	121.5
$C_3{-}C_{3a}{-}C_{9b}$	118.8	118.4	119.3
$C_4{-}C_{3a}{-}C_{9b}$	119.4	118.9	120.0
$C_{3a}{-}C_4{-}C_5$	120.7	120.4	121.2
$C_4{-}C_5{-}C_6$	120.4	120.8	119.9
$C_5{-}C_6{-}C_{6a}$	120.4	120.4	120.4
$C_6{-}C_{6a}{-}C_{9b}$	119.3	118.9	120.2
$C_7{-}C_{6a}{-}C_{9b}$	118.5	118.4	118.5
C_{6a}-$C_7{-}C_8$	121.2	122.0	120.4
$C_7{-}C_8{-}C_9$	120.4	120.4	121.4
$C_8{-}C_9{-}C_{9a}$	120.0	118.1	120.5
$C_9{-}C_{9a}{-}C_{9b}$	119.6	121.3	118.2
$C_1{-}C_{9a}{-}C_{9b}$	121.0	121.3	120.0
$C_2{-}C_1{-}C_{9a}$	116.8	118.1	116.0
$C_{3a}{-}C_{9b}{-}C_{9a}$	120.0	119.7	120.6
$C_{3a}{-}C_{9b}{-}C_{6a}$	119.7	120.6	118.3
$C_{6a}{-}C_{9b}{-}C_{9a}$	120.3	119.7	121.1
$O_{10}{-}C_1{-}C_{9a}$	121.6	119.8	123.5
$O_{11}{-}C_9{-}C_{9a}$	121.9	119.8	119.9
$C_9{-}O_{11}{-}H$	104.9	101.3	107.7
$C_1{-}C_2{-}H$	116.8	118.0	115.6
$C_{3a}{-}C_3{-}H$	118.0	118.3	118.0
$C_{3a}{-}C_4{-}H$	119.2	119.3	118.8
$C_4{-}C_5{-}H$	119.7	119.6	119.9
$C_{6a}{-}C_6{-}H$	119.1	119.3	118.8
$C_{6a}{-}C_7{-}H$	118.8	118.3	119.5
$C_7{-}C_8{-}H$	121.6	121.6	120.0

[a] Calculated at the MP2/6−311(++)G** level; for details see text.

Variation of the bond angles in the hydrogen-bonded moiety can be attributed to the turn of the OH group resulting in a change from attractive (**1a**) to repulsive steric interactions (**1c**). Thus in **1a** the $C_9{-}O_{11}{-}H$ and $C_{9a}{-}C_1{-}O_{10}$ angles are smaller by 2.8 and 1.9°, respectively, in agreement with the shorter O··· O distance. Differences in the phenalene skeleton angles are much smaller, they are generally within 1°. The characteristic changes in the geometrical parameters upon HB are in agreement

with those found for the atomic charges (vide supra) and show that the variation of the electron density distribution associated with a formation of HB in that strongly conjugated system is concentrated in the hydrogen-bonded moiety.

The symmetric form **1b** reflects the increase of resonance effects discussed above in the relation of **1a** and **1c**. Besides the equalization of the two C−O bond lengths, most pronounced is the further shortening of C_1-C_{9a} and C_1-C_2 by 0.036 and 0.019 Å, respectively, and the lengthening of C_8-C_9 and C_9-C_{9a} in a similar amount. Most of the other C−C bonds alter by ca. 0.01 Å with respect to those in **1a**, indicating considerable electron density redistribution when going to the symmetric hydrogen-bonded form. The strengthening of the HB interaction is manifested by the 2.369 Å long O···O distance, shortened by 0.17 Å with respect to that in **1a**. Among the bond angles again the change in the hydrogen-bonded moiety is the most significant (see, e.g., the decrease of the $C_9-O_{11}-H$ and $C_{9a}-C_1-O_{10}$ angles by 3.6° and 1.8°, respectively). The O···H···O angle is 160.5° in **1b** (cf. Table 1), increased toward linearity by 8° from **1a**.

The CH bond distances and CCH angles are practically unchanged during the **1c**−**1a**−**1b** interconversion, except for C_8-H affected by a steric interaction with the OH hydrogen in **1c**.

The above results confirm the suggested[34] substantial structural reorganization between the equilibrium configurations (**1a**, **1c**) and the transition state (**1b)**, most of the changes in interatomic distances and bond angles being localized in the proximity of the hydrogen bond.

We note the performance of the present DFT methods for the geometrical parameters of **1**. As was seen at the selected geometrical characteristics of the hydrogen bond (Table 1), the B3-LYP geometrical parameters show very similar features to those of MP2, while the B3-P86 ones carry more the consequences of the overestimated HB interaction.

At a joint analysis of calculated and experimental[23] molecular geometries first of all the different physical meaning of the two sets of data should be taken into account.[69] Whereas the quantum chemical calculations provide a straightforward picture of the geometry at the bottom of the minimum of the PES, experimental observations pertain instead to a dynamic average. The X-ray diffraction experiment samples in the space over many pseudostatic atomic configurations due to the short interaction time between the X-ray photon and the molecule. This interaction time is by several orders of magnitude shorter than the molecular vibrations including the tunneling motion. Thus, in the case of **1** the X-ray diffraction method can be expected to provide a statistical correlation between the oxygen−oxygen distance and the position of the hydrogen in the hydrogen bridge. The experimental data reflect additionally the effects of intermolecular interactions in the solid phase while the computations model the free molecule.

In agreement with the above comments the X-ray diffraction experiment resulted in a structure intermediate between **1a** and **1b**.[23] The experimental geometrical parameters can be well correlated with the changes in the molecular geometry during proton tunneling in the double minimum potential well (vide supra). We note the near C_{2v} symmetry of the X-ray structure where most of the mirror bond distance and bond angle counterparts (separated by the vertical plane of symmetry of **1b**) agree within experimental error.[23]

2. Vibrational Analysis. The FT-IR and FT-Raman spectra of 9-hydroxyphenalen-1-one are shown in Figure 2, while the calculated vibrational data of the global minimum **1a** structure

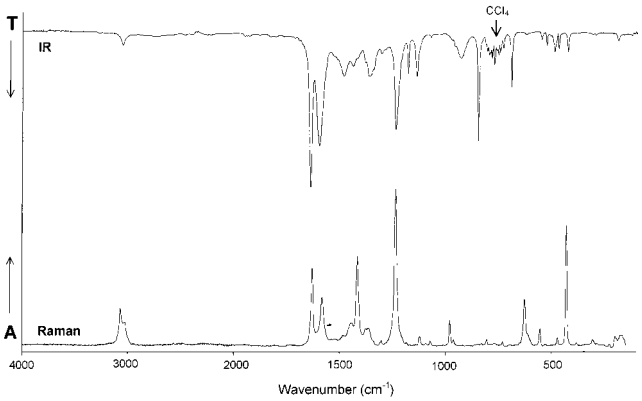

Figure 2. FT-IR (top, 0.05 M CCl_4 solution) and FT-Raman (bottom, solid) spectra of 9-hydroxyphenalen-1-one. (T = transmittance, A = Raman activity).

are included into Table 3. The experimental spectra reflect the characteristics of the calculated vibrational frequencies and the IR and Raman activities of **1a**, providing another support for the double minimum potential well.

The interpretation of the experimental spectra was based on the scaled computed B3-LYP/6−311(++)G** force field utilizing additional information from computed (unscaled) IR intensities and Raman activities. The choice of the B3-LYP force field is reasoned by the found good agreement between the MP2 and B3-LYP results for the HB interaction and geometrical parameters of **1a**.

Our scaling procedure was determined by the fact that selective scale factors for B3-LYP/6−311(++)G** force fields were not available at the start of our study. At the first stage of our analysis we used the scale factors of Baker et al. developed for B3-LYP/6-31G* force fields.[70] Despite the differences between the two theoretical levels this initial set of scale factors performed rather well for **1a** and resulted in an rms deviation of 12.6 cm^{-1} between the scaled and observed fundamental frequencies. This good performance is a consequence of the good quality of vibrational frequencies computed by DFT.[71]

The only very large deviation was found for the OH torsional mode ($\Delta\nu = 54$ cm^{-1}, not included in the rms statistics). This deficiency for the OH torsion is in agreement with experience that general scale factors for the vibrations of hydrogen-bonded OH groups cannot be developed at the B3-LYP/6-31G* level.[60,72−74] This valence double-ζ basis set was shown to be insufficient for HB interactions[36,59,60] resulting in a sensitivity of the calculated OH vibrational frequencies on the type (strength) of HB. This means that the errors of these computed force fields for the hydrogen-bonded OH vibrations are not systematic in contrast to the other vibrations of common organic molecules. This deficiency may vanish using larger basis sets.

In the second stage of our analysis we optimized the scale factors for **1a**. This was necessary to obtain the most reliable characterization of the fundamentals as well as to develop a set of scale factors specifically for **1**. The optimized set can be used additionally for the vibrational analysis of the non-hydrogen-bonded form **1c** with the goal to obtain information on the change of mixing of internal coordinates upon the strong HB interaction. Those scale factors from ref 70 that worked sufficiently well for **1a** were kept at their original value, while the other ones (referring mainly for the OH group and skeletal vibrations) were optimized on the basis of the available experimental data. The reliability of our final scaled force field was supported by its good performance for the deuteriohydroxy derivative **1a**−d. The final set of scale factors is given in Table

TABLE 3: Fundamental Vibrational Frequencies (cm^{-1}) of 9-Hydroxyphenalen-1-one (1a)[a]

			calcd		
	ν	exp[b]	unscaled[c]	scaled	characterization
A′	1	3072 m[d]	3200 (5; 220)	3063	100% CH st
	2		3196 (7; 209)	3060	100% CH st
	3	3050 w	3192 (22; 297)	3056	100% CH st
	4	3028 sh	3171 (19; 192)	3035	100% CH st
	5		3168 (1; 68)	3032	100% CH st
	6		3164 (3; 46)	3029	100% CH st
	7		3157 (7; 62)	3022	100% CH st
	8		2994 (228; 49)	2994	98% OH st
	9	1639 s	1674 (393; 167)	1634	57% CC st, 20% CCC b, 12% CH b, 10% C═O st
	10	1606 sh	1642 (107; 30)	1598	45% CC st, 27% C═O st, 16% CH b, 11% CCC b
	11	1597 s	1636 (137; 2)	1591	68% CC st, 18% CH b, 11% CCC b
	12	1579 sh	1628 (89; 117)	1579	58% CC st, 17% OH b, 13% CCC b
	13	1538 w[d]	1595 (9; 19)	1549	51% CC st, 21% C═O st, 18% CH b, 10% OH b
	14	1507 w	1526 (20; 45)	1490	55% CC st, 35% CH b
	15	1482 s	1520 (154; 8)	1476	43% CC st, 22% CH b, 17% OH b
	16	1439 m	1467 (44; 36)	1436	54% CH b, 28% CC st
	17	1417 sh	1442 (1; 71)	1411	50% CH b, 37% CC st
	18	1383 sh	1434 (18; 34)	1395	67% CC st, 18% CH b
	19	1365 m	1412 (68; 15)	1375	33% CC st, 24% CH b, 17% CO st, 14% CCC b
	20	1355 sh	1401 (6; 32)	1367	60% CC st, 17% CH b, 10% CCC b
	21	1342 m	1371 (68; 12)	1333	62% CC st, 14% CH b
	22	1305 w	1334 (66; 6)	1302	44% CO st, 25% CC st, 23% CH b
	23		1265 (13; 73)	1239	48% CH b, 41% CC st, 10% CCC b
	24	1238 s	1262 (175; 108)	1226	53% CC st, 25% CH b, 13% OH b
	25	1212 sh	1245 (9; 2)	1218	52% CC st, 36% CH b
	26	1181 m	1204 (19; 2)	1182	69% CH b, 31% CC st
	27	1140 m	1166 (46; 6)	1145	66% CH b, 32% CC st
	28	1124 w	1144 (3; 7)	1123	55% CH b, 32% CC st, 10% CCC b
	29	1097 w[d]	1127 (<1; 3)	1105	41% CC st, 31% CCC b, 25% CH b
	30	1073 w	1100 (3; 10)	1074	60% CC st, 30% CH b
	31	977 w	995 (2; 12)	975	43% CCC b, 42% CC st
	32	961 sh	979 (5; 6)	953	73% CC st, 12% CCC b
	33	807 w[d]	821 (3; 3)	810	72% CCC b, 23% CC st
	34		747 (2; 2)	736	67% CCC b, 27% CC st
	35		743 (5; 1)	729	46% CCC b, 43% CC st
	36	625 w	634 (7; 37)	619	56% CC st, 34% CO b
	37	553 w	565 (4; 20)	551	65% CC st, 19% CCC b, 14% CO b
	38	530 w	542 (6; 2)	535	73% CCC b, 13% CC st, 10% CO b
	39	491 m	496 (19; <1)	490	46% CCC b, 41% CO b, 11% CC st
	40	430 w	436 (8; 25)	429	64% CCC b, 32% CC st
	41		430 (2; 6)	423	55% CCC b, 29% CC st, 13% CO b
	42	384 w[e]	388 (<1; <1)	382	57% CCC b, 28% CC st, 12% CO b
	43	314 w[e]	326 (8; 1)	321	42% CCC b, 32% CO b, 24% CC st
A"	44	996 w[d]	1005 (<1; 2)	996	100% CH wag
	45		991 (1; <1)	982	100% CH wag
	46		981 (0; <1)	971	100% CH wag
	47	932 s	963 (95; <1)	932	98% OH t
	48		932 (0; 1)	921	100% CH wag
	49	850 s	866 (87; ∼0)	855	70% CH wag, 23% CO wag
	50	833 w	846 (3; 1)	836	82% CH wag, 16% CO wag
	51		803 (<1; <1)	789	44% CH wag, 35% CC t, 21% CO wag
	52	736 w[e]	760 (15; 15)	747	49% CH wag, 46% CC t
	53	700 sh	713 (9; <1)	698	64% CC t, 27% CO wag
	54	694 m	698 (13; <1)	685	55% CC t, 35% CO wag, 10% CH wag
	55		552 (0; <1)	539	95% CC t
	56		544 (<1; 2)	534	62% CC t, 29% CO wag
	57	473 w	480 (5; 4)	468	100% CC t
	58	385 w[d]	389 (0; 1)	380	90% CC t, 10% CO wag
	59	299 w[e]	300 (1; <1)	293	85% CC t, 15% CO wag
	60		219 (0; ∼0)	213	100% CC t
	61	193 w	188 (4; <1)	183	95% CC t
	62		131 (<1; 1)	128	100% CC t
	63		109 (1; 1)	107	100% CC t

[a] The abbreviations s, m, w, and sh mean strong, medium, weak, and shoulder, while st, b, wag, and t mean stretching, bending, wagging, and torsion, respectively. [b] From the IR spectrum of 0.05 M CCl_4 solution except where noted. [c] Calculated at the B3-LYP/6−311(++)G** level; for details see text. Calculated IR intensities (km/mol) and Raman activities ($Å^4$/amu) in parentheses. [d] From the Raman spectrum of the solid. [e] From the IR spectrum of the solid.

4. We note that the new scale factors of Set2 are generally somewhat closer to unity than the ones of Baker et al.[70] developed for the smaller 6-31G* basis set. With the optimized scale factors rms deviations of 6.9 and 6.7 cm^{-1} were achieved between the SQM and experimental frequencies of **1a** (45 fundamentals) and **1a**−d (36 fundamentals), respectively.

TABLE 4: Scale Factors Used in the SQM Analysis

mode	Set1[a]	Set2
CC stretching	0.9207	0.9398[b]
CO stretching	0.9207	0.9497[b]
CH stretching	0.9164	0.9164
OH stretching	0.9200	1.0000
CCC bending	1.0144	0.9844[b]
CO bending	1.0144	0.9722[b]
CH bending	0.9431	0.9748[b]
OH bending	0.8760	0.8896[b]
CO wagging	0.9760	0.9760
CH wagging	0.9760	0.9760
CC torsion	0.9523	0.9523
OH torsion	0.9350	0.9350

[a] From ref 70. [b] Optimized in the present study.

The results of our SQM analysis for **1a** are given in Table 3. From a point of view of the strong intramolecular HB most important are the vibrations of the OH group. Experimental support to the assignment of these fundamentals was provided by the IR spectrum of **1a**−d.

Most characteristic on the strong low-barrier HB in **1a** is the absence of the OH stretching band in the experimental IR spectrum. The absence of this band is a general spectral feature of enolized β-diketones attributed to the electron configuration of the chelate ring.[75] The charge-transfer contribution to the (usually high) intensity of a hydrogen-bonded OH stretching band may be, in the conjugate rings, compensated by electronic shifts in the rings and thus the dipole moment change with the proton vibration is small. Indeed, the calculated natural charges indicate an opposite shift of the positive charge in the chelate ring when the proton moves between the oxygens (cf. the NBO charges of C_1 and C_9 in Table 1). However, such a considerable intensity decrease of the OH stretching band is not reflected by the calculations. Calculated IR intensities in the same magnitude (200−400 km/mol) were obtained for other intramolecular HB systems with strong ν_{OH} bands in their IR spectra.[60,73,74] On the other hand, the harmonic approximation used in the frequency calculations may be completely inadequate for this strongly anharmonic fundamental of **1a**.

Another reason of the absence of the ν_{OH} band may be that we face an IR continuum in the spectrum. Such a phenomenon arises when either the ground or an excited state (or both) of the proton tunneling motion have a continuous energy level distribution.[76] This continuity of energy level differences appears with easily polarizable hydrogen bonds and is caused by various interactions of the hydrogen bond with the environment. Most important from these interaction effects are the induced dipole interactions between the hydrogen bonds, mutual interactions via proton dispersion forces, a coupling of the proton tunneling with the bond stretching and other intermolecular vibrations. Additionally, a characteristic feature of amorphous systems is the large distribution of the equilibrium bond length of these polarizable hydrogen bonds.

The B3-LYP calculations predict an OH stretching frequency of 2994 cm^{-1}. This, however, must be considerably overestimated as a result of the harmonic approximation. In the case of the very flat and anharmonic PES around the global minimum in such strong HB systems[77] an anharmonic treatment of the OH stretching motion would be necessary to describe this vibration properly. The anharmonicity of the PES was studied in $XH\cdots NY_3$ (X = Cl, Br; Y = H, CH_3) molecules including both traditional and short-strong hydrogen bonds, partly with experimental information available. The anharmonic XH stretching frequencies were found to be lower by 500−1000 cm^{-1} than the computed harmonic frequencies.[77,78] Based on the close relation of the PES in these strong HB systems with that in **1**, the stretching frequency of the OH proton in **1a** may be expected in the range 1800−2500 cm^{-1}.

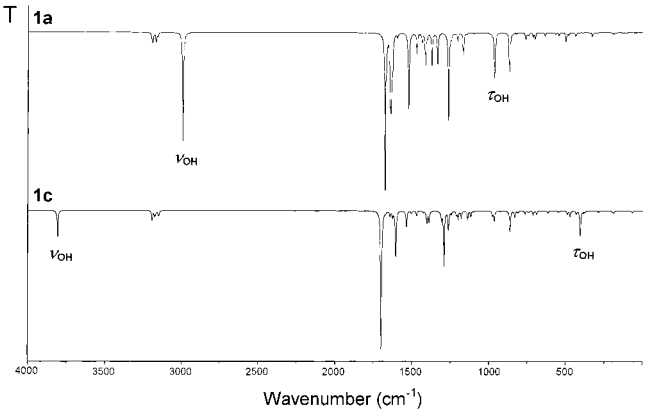

Figure 3. Computed (unscaled) IR spectra of the two characteristic structures **1a** and **1c**.

A possible mixing of the OH stretching mode with other vibrations was investigated by gradually scaling down its frequency within the expected range.[79] The mixing started to be significant only below 2000 cm^{-1}. The main contributions to the total energy distribution (TED) were 90% OH stretch and 7% OH bend at 2000 cm^{-1}, while it changed to 81% OH stretch, 13% OH bend, and 4% CO bend at 1800 cm^{-1}. The rms deviation between the scaled and experimental frequencies increased by only 0.1 cm^{-1} during this procedure and the TED of the other normal modes changed in a negligible amount. Hence we can expect that the results of our SQM analysis given in Table 3 represent a reliable description of the vibrational properties of **1a**.

In contrast to OH stretching, the bands of the OH torsional and bending vibrations can be observed in the experimental spectra. Among them the best defined is the torsional mode at 932 cm^{-1} (TED: 98% OH torsion, cf. Table 3). Its very high frequency is another experimental clue of the strong HB in **1a**. The OH bending vibration is less characteristic. It is distributed among several fundamentals being a minor component in ν_{12}, ν_{13}, ν_{15}, and ν_{24}. A similar feature can be observed for the C═O stretching vibration being distributed among ν_9, ν_{10}, and ν_{13}. Such an intense mixing of the C═O stretch with skeletal vibrations is characteristic for strongly conjugated systems.[80,81] Our results support the assignment of Fernández-Ramos et al.[34] for ν_{36}, ν_{39}, and ν_{43}, involving a large contribution of CO bending.

Because of its much lower stability the non-hydrogen-bonded **1c** form cannot be observed experimentally. It is, however, an interesting question to what extent the molecular properties of **1a** come from the strongly conjugated phenalenone skeleton and what can be attributed to the strong intramolecular HB. This can be deduced only by comparing the computed parameters of the two conformers, as was done in the previous section with the molecular geometries. For an analogous analysis of the vibrational properties, we performed an SQM analysis of **1c** using the scale factors optimized for **1a**. The calculated IR spectra of **1a** and **1c** are depicted in Figure 3. Besides the obviously different frequencies of the OH stretching and torsional modes, most characteristic is the enhanced IR intensity of several fundamentals of **1a** with respect to these in the spectrum of **1c**. This is in agreement with the previously discussed increased charge separations upon the HB interaction, resulting in a larger dipole moment change during the vibrations.

Another effect of HB is the very strong mixing of the CO and OH vibrations both with each other and with the skeletal vibrations in **1a**.

Conclusions

The hydrogen bond in 9-hydroxyphenalen-1-one presents several properties characteristic for strong low-barrier HBs:

—an enhanced strength relative to traditional hydrogen bonds

—a computed double-minimum potential energy surface with a low (ca. 10 kJ/mol) barrier, in agreement with the experimentally observed proton tunneling

—a short distance between the hydrogen-donor and the hydrogen-acceptor atoms

—a very high OH torsional (932 cm^{-1}) and a computed very low OH stretching frequency, where the latter band shows a continuum in both the IR and Raman spectra

The HB energy in **1a** was estimated to be ca. 60 kJ/mol. On the basis of a joint analysis of the energetics and molecular geometry, the HB interaction can be classified as a border case between traditional and short-strong hydrogen bonds. The molecule undergoes substantial structural reorganization between the equilibrium configuration and the transition state, most of the changes in interatomic distances and bond angles being localized in the area of the oxygen atoms.

The charge distribution refers to the predominantly ionic character of the HB interaction with marginal differences between the asymmetric (**1a**) and symmetric (**1b**) forms. The increased charge separation in the keto−enol moiety upon HB is reflected in the enhanced IR intensities of several fundamentals. Another characteristic effect of HB on the vibrational properties of **1** is the enhanced mixing of the CO and OH vibrations with each other and with the skeletal modes.

Our comparative study of the three theoretical levels (MP2, B3-LYP, B3-P86) revealed the very good performance of the B3-LYP density functional in conjunction with a diffuse polarized valence triple-ζ basis set while the B3-P86 functional tends to overestimate considerably the strong hydrogen-bonding interaction.

The assignment of the vibrational spectra was based on a scaled quantum mechanical (SQM) treatment of the computed B3-LYP/6−311(++)G** force field utilizing 11 scale factors. As a result of the SQM analysis, 45 from a total of 63 fundamentals of **1a** were assigned with an rms deviation of 6.9 cm^{-1} between the experimental and scaled frequencies.

Acknowledgment. A.K. thanks gratefully the Japan International Science&Technology Exchange Center (JISTEC) for an STA fellowship and the Hungarian Scientific Research Foundation (OTKA No. T030053) and the Bolyai Foundation for finantial support. Prof. G. Keresztury is thanked for the Raman spectrum.

References and Notes

(1) Jeffrey, G. A. *An Introduction to Hydrogen Bonding*; Oxford University Press: Oxford, U.K., 1997.

(2) Del Bene, J. E. Hydrogen Bonding: 1. In *Encyclopedia of Computational Chemistry*; Schleyer, P. v. R., Allinger, N. L., Clark, T., Gasteiger, J., Kollman, P. A., Schaefer, H. F., III, Schreiner, P. R., Eds.; J. Wiley and Sons: Chichester, U.K., 1998; Vol. 2, pp 1263−1271.

(3) Hibbert, F.; Emsley, J. *Adv. Phys. Org. Chem.* **1990**, *26*, 255.

(4) Emsley, J. *Chem. Soc. Rev.* **1980**, *9*, 91.

(5) Shan, S.; Loh, S.; Herschlag, D. *Science* **1996**, *272*, 97.

(6) Schwartz, B.; Drueckhammer, D. G. *J. Am. Chem. Soc.* **1995**, *117*, 11902.

(7) Wesolowski, T.; Muller, R. P.; Warshel, A. *J. Phys. Chem.* **1996**, *100*, 15444.

(8) Scheiner, S.; Yi, M. *J. Phys. Chem.* **1996**, *100*, 9235.

(9) Laidig, K. E.; Platts, J. A. *J. Phys. Chem.* **1996**, *100*, 13455.

(10) Garcia-Viloca, M.; Gonzalez-Lafont, A.; Lluch, J. M. *J. Am. Chem. Soc.* **1997**, *119*, 1081.

(11) McAllister, M. A. *Can. J. Chem.* **1997**, *75*, 1195.

(12) Madsen, G. K. H.; Wilson, C.; Nymand, T. M.; McIntyre, G. J.; Larsen, F. K. *J. Phys. Chem. A* **1999**, *103*, 8684.

(13) Benoit, M.; Marx, D.; Parrinello, M. *Nature* **1998**, *392*, 258.

(14) Loubeyre, P.; LeToullec, R.; Wolanin, E.; Hanfland, M.; Hausermann, D. *Nature* **1998**, *397*, 503.

(15) Cleland, W. W. *Biochemistry* **1992**, *31*, 317.

(16) Warshal, A.; Papazyan, A.; Kollman, P. A. *Science* **1995**, *269*, 102.

(17) Cleland, W. W.; Kreevoy, M. M. *Science* **1994**, *264*, 1927.

(18) Wesolowski, T.; Muller, R. P.; Warshel, A. *J. Phys. Chem.* **1996**, *100*, 15444.

(19) Guthrie, J. P. *Chem. Biol.* **1996**, *3*, 163.

(20) Emsley, J. *Struct. Bond.* **1984**, *57*, 147.

(21) Gilli, G.; Bellucci, F.; Ferretti, V.; Bertolasi, V. *J. Am. Chem. Soc.* **1989**, *111*, 1023.

(22) Gilli, P.; Ferretti, V.; Bertolasi, V.; Gilli, G. In *Advances in Molecular Structure Research*; Hargittai, M., Hargittai, I., Eds.; JAI Press: Greenwich, CT, 1996; Vol. 2, pp 67−102.

(23) Svensson, C.; Abrahams, S. C.; Bernstein, J. L.; Haddon, R. C. *J. Am. Chem. Soc.* **1979**, *101*, 5759.

(24) Demura, Y.; Kawato, T.; Kanatomi, H.; Murase, I. *Bull. Chem. Soc. Jpn.* **1975**, *48*, 2820.

(25) Svensson, C.; Abrahams, S. C. *Acta Crystallogr.* **1986**, *B42*, 280.

(26) Brown, R. S.; Tse, A.; Nakashima, T.; Haddon, R. C. *J. Am. Chem. Soc.* **1979**, *101*, 3157.

(27) Engdahl, C.; Gogoll, A.; Edlund, U. *Magn. Reson. Chem.* **1991**, *29*, 54.

(28) Jackman, L. M.; Trewella, J. C.; Haddon, R. C. *J. Am. Chem. Soc.* **1980**, *102*, 2519.

(29) Rossetti, R.; Haddon, R. C.; Brus, L. E. *J. Am. Chem. Soc.* **1980**, *102*, 6913.

(30) Bondybey, V. E.; Haddon, R. C.; English, J. H. *J. Chem. Phys.* **1984**, *80*, 5432.

(31) Kunze, K. L.; de la Vega, J. R. *J. Am. Chem. Soc.* **1984**, *106*, 6528.

(32) Ozeki, H.; Takahashi, M.; Okuyama, K.; Kimura, K. *J. Chem. Phys.* **1993**, *99*, 56.

(33) Sekiya, H.; Nakano, N.; Nishi, K.; Hamabe, H.; Sawada, T.; Tashiro, M.; Nishimura, Y. *Chem. Lett.* **1995**, 893.

(34) Fernández-Ramos, A.; Smedarchina, Z.; Zgierski, M. Z.; Siebrand, W. *J. Chem. Phys.* **1998**, *109*, 1004.

(35) Møller, C.; Plesset, M. S. *Phys. Rev.* **1934**, *46*, 618.

(36) Del Bene, J. E.; Person, W. B.; Szcepaniak, K. *J. Phys. Chem.* **1995**, *99*, 10705.

(37) Lozynski, M.; Rusinska-Roszak, D.; Mack, H.-G. *J. Phys. Chem. A* **1998**, *102*, 2899.

(38) Jordan, M. J. T.; Del Bene, J. E. *J. Am. Chem. Soc.* **2000**, *122*, 2101.

(39) Eckert-Maksic, M.; Maksic, Z. B.; Margetic, D. *Croat. Chem. Acta* **1989**, *62*, 645.

(40) Rodríguez, J. *J. Comput. Chem.* **1994**, *15*, 183.

(41) Feng, J.; Liu, T.; Li, Z. *Gaodeng Xuexiao Huaxue Xuebao* **1991**, *12*, 494.

(42) Orlov, V. D.; Solodar, S. L.; Surov, Yu. N.; Vinogradov, L. M.; Chistova, S. E. *Zh. Org. Khim.* **1982**, *18*, 615.

(43) Jayaraman, A.; Kourouklis, G. A.; Haddon, R. C. *J. Chem. Phys.* **1987**, *87*, 3587.

(44) Becke, A. D. *J. Chem. Phys.* **1993**, *98*, 5648.

(45) Lee, C.; Yang, W.; Parr, R. G. *Phys. Rev. B* **1988**, *37*, 785.

(46) Perdew, J. P. *Phys. Rev. B* **1986**, *33*, 8822.

(47) Frisch, M. J.; Trucks, G. W.; Schlegel, H. B.; Scuseria, G. E.; Robb, M. A.; Cheeseman, J. R.; Zakrzewski, V. G.; Montgomery, J. A., Jr.; Stratmann, R. E.; Burant, J. C.; Dapprich, S.; Millam, J. M.; Daniels, A. D.; Kudin, K. N.; Strain, M. C.; Farkas, O.; Tomasi, J.; Barone, V.; Cossi, M.; Cammi, R.; Mennucci, B.; Pomelli, C.; Adamo, C.; Clifford, S.; Ochterski, J.; Petersson, G. A.; Ayala, P. Y.; Cui, Q.; Morokuma, K.; Malick, D. K.; Rabuck, A. D.; Raghavachari, K.; Foresman, J. B.; Cioslowski, J.; Ortiz, J. V.; Stefanov, B. B.; Liu, G.; Liashenko, A.; Piskorz, P.; Komaromi, I.; Gomperts, R.; Martin, R. L.; Fox, D. J.; Keith, T.; Al-Laham, M. A.; Peng, C. Y.; Nanayakkara, A.; Gonzalez, C.; Challacombe, M.; Gill, P. M. W.; Johnson, B.; Chen, W.; Wong, M. W.; Andres, J. L.; Gonzalez, C.; Head-Gordon, M.; Replogle, E. S.; Pople, J. A. *Gaussian98*, revision A.6; Gaussian, Inc.: Pittsburgh, PA, 1998.

(48) Pulay, P.; Fogarasi, G.; Pongor, G.; Boggs, J. E.; Vargha, A. *J. Am. Chem. Soc.* **1983**, *105*, 7037.

(49) Coffin, J. M.; Pulay, P. Program TRA3, Department of Chemistry and Biochemistry, University of Arkansas, Fayetteville, AR, 1989.

(50) Pulay, P. In *Applications of Electronic Structure Theory*, *Modern Theoretical Chemistry*, Schaefer, H. F., III, Ed.; Plenum: New York, 1977; Vol. 4, p 153.

(51) Pongor, G.; Fogarasi, G.; Magdó, I.; Boggs, J. E.; Keresztury, G.; Ignatyev, I. S. *Spectrochim. Acta* **1992**, *48A*, 111.
(52) Pongor, G. Program SCALE3, Department of Theoretical Chemistry, Eötvös Loránd University, Budapest, Hungary, 1993.
(53) Pulay, P.; Török, F. *Acta Chim. Hung.* **1965**, *44*, 287.
(54) Keresztury, G.; Jalsovszky, G. *J. Mol. Struct.* **1971**, *10*, 304.
(55) Koelsch, C. F.; Anthes, J. A. *J. Org. Chem.* **1941**, *6*, 558.
(56) The character of the spectra did not change upon further dilution.
(57) Wenthold, P.; Squires, R. *J. Phys. Chem.* **1995**, *99*, 2002.
(58) Isaacson, A. D.; Morokuma, K. *J. Am. Chem. Soc.* **1975**, *97*, 4453.
(59) Kovács, A.; Csonka, G. I., Kolossváry, I.; Hargittai, I. *J. Comput. Chem.* **1996**, *17*, 1804.
(60) Macsári, I.; Izvekov, V.; Kovács, A. *Chem. Phys. Lett.* **1997**, *269*, 393.
(61) Madsen, G. K. H.; Wilson, C.; Nymand, T. M.; McIntyre, G. J.; Larsen, F. K. *J. Phys. Chem. A* **1999**, *103*, 8684.
(62) Reed, A. E.; Curtiss, L. A.; Weinhold, F. *Chem. Rev.* **1988**, *88*, 899.
(63) Jönsson, P. G.; Hamilton, W. C. *J. Chem. Phys.* **1972**, *56*, 4433.
(64) Leviel, J.-L.; Auvert, G.; Savariault, J. M. *Acta Crystallogr. B* **1981**, *37*, 2185.
(65) Jönsson, P. G. *Acta Crystallogr. B* **1971**, *27*, 893.
(66) Ellison, R. D.; Johnson, C. K.; Levy, H. A. *Acta Crystallogr. B* **1971**, *27*, 333.
(67) Jönsson, P. G. *Acta Chem. Scand.* **1972**, *26*, 1599.
(68) Ichikawa, M. *Acta Crystallogr. B* **1978**, *34*, 2074.
(69) Hargittai, M.; Hargittai, I. *Int. J. Quantum Chem.* **1992**, *44*, 1057.
(70) Baker, J.; Jarzecki, A. A.; Pulay, P. *J. Phys. Chem. A* **1998**, *102*, 1412.
(71) Jensen, F. *Introduction to Computational Chemistry*; Wiley & Sons: New York, 1999; p 188.
(72) Rauhut, G.; Pulay, P. *J. Phys. Chem.* **1995**, *99*, 3093.
(73) Kovács, A.; Izvekov, V.; Keresztury, G.; Pongor, G. *Chem. Phys.* **1998**, *238*, 231.
(74) Kovács, A.; Keresztury, G.; Izvekov, V. *Chem. Phys.* **2000**, *253*, 193.
(75) Hadži, D.; Bratos, S. In *The Hydrogen Bond*; Schuster, P., Zundel, G., Sandorfy, C., Eds.; North-Holland Publishing Co.: Amsterdam, 1976; Chapter 12.5, p 603.
(76) Zundel G. In *The Hydrogen Bond*; Schuster, P., Zundel, G., Sandorfy, C., Eds.; North-Holland Publishing Co.: Amsterdam, 1976; Chapter 15.5, p 728.
(77) Jordan, M. J. T.; Del Bene, J. E. *J. Am. Chem. Soc.* **2000**, *122*, 2101.
(78) Barnes, A. J.; Wright, M. P. J. *J. Chem. Soc., Faraday Trans. 2* **1986**, *82*, 153.
(79) All the other scale factors (Set2 in Table 3) were kept constant. The off-diagonal force constants vary as $f_{ij}' = (t_i t_j)^{1/2} f_{ij}$ (t is the scale factor for the diagonal force constants), which introduces an empirical character into our procedure.
(80) Kovács, A.; Szabó, A. *J. Mol. Struct.* **1999**, *510*, 215.
(81) Avbelj, F.; Hodošček, M.; Hadži, D. *Spectrochim. Acta* **1985**, *41A*, 89.